

# Selection Bias in Observing the Cosmological Evolution of the $M_{\bullet} - \sigma$ and $M_{\bullet} - L$ Relationships

Tod R. Lauer

*National Optical Astronomy Observatory<sup>1</sup>, P.O. Box 26732, Tucson, AZ 85726*

Scott Tremaine

*Institute for Advanced Study, Einstein Drive, Princeton, NJ 08540*

Douglas Richstone

*Department of Astronomy, University of Michigan, Ann Arbor, MI 48109*

S. M. Faber

*UCO/Lick Observatory, Board of Studies in Astronomy and Astrophysics, University of California, Santa Cruz, CA 95064*

## ABSTRACT

Programs to observe evolution in the  $M_{\bullet} - \sigma$  or  $M_{\bullet} - L$  relations typically compare black-hole masses,  $M_{\bullet}$ , in high-redshift galaxies selected by nuclear activity to  $M_{\bullet}$  in local galaxies selected by luminosity  $L$ , or stellar velocity dispersion  $\sigma$ . Because AGN luminosity is likely to depend on  $M_{\bullet}$ , selection effects are different for high-redshift and local samples, potentially producing a false signal of evolution. This bias arises because cosmic scatter in the  $M_{\bullet} - \sigma$  and  $M_{\bullet} - L$  relations means that the mean  $\log_{10} L$  or  $\log_{10} \sigma$  among galaxies that host a black hole of given  $M_{\bullet}$ , may be substantially different than the  $\log_{10} L$  or  $\log_{10} \sigma$  obtained from inverting the  $M_{\bullet} - L$  or  $M_{\bullet} - \sigma$  relations for the same nominal  $M_{\bullet}$ . The bias is particularly strong at high  $M_{\bullet}$ , where the luminosity and dispersion functions of galaxies are falling rapidly. The most massive black holes occur more often as rare outliers in galaxies of modest mass than in the even rarer high-mass galaxies, which would otherwise be the sole location of such black holes in the absence of cosmic scatter. Because of this bias,  $M_{\bullet}$  will typically appear to be too large in the distant sample for a given  $L$  or  $\sigma$ . For the largest black holes and the largest plausible cosmic scatter, the bias can reach a factor of 3 in  $M_{\bullet}$  for the  $M_{\bullet} - \sigma$  relation and a factor of 9 for the  $M_{\bullet} - L$  relation. Unfortunately, the actual cosmic scatter is not known well enough to correct for the bias. Measuring evolution of the  $M_{\bullet}$  and galaxy property relations requires object selection to be precisely defined and exactly the same at all redshifts.

*Subject headings:* galaxies: nuclei — Galaxies: Evolution — Galaxies: Fundamental Parameters

## 1. Observing Evolution in the Relationships Between Black Hole Mass and Galaxy Properties

The discovery that most elliptical galaxies and spiral bulges host a black hole at their centers, plus the tight relations observed between black-hole mass  $M_{\bullet}$  and galaxy luminosity  $L$  or stellar velocity dispersion  $\sigma$  (Dressler 1989; Kormendy 1993; Kormendy & Richstone 1995; Magorrian et al. 1998; Ferrarese & Merritt 2000; Gebhardt et al. 2000a; Tremaine et al. 2002; Häring & Rix 2004), suggest that the formation and growth of central black holes is deeply intertwined with that of their host galaxies. Recent theoretical work (e.g., Hopkins et al. 2006) supports this view, and also predicts how the relations between the properties of black holes and their host galaxies have changed over time. Direct observation of the evolution of the  $M_{\bullet} - \sigma$  and  $M_{\bullet} - L$  relations over cosmological time would offer unique insight into galaxy and black-hole formation.

There have been many attempts to measure the evolution of the  $M_{\bullet}$  relations; we cite a partial list of these:

- Shields et al. (2003) examine a sample of quasars at redshifts up to 3.3. The luminosity  $L$  and velocity dispersion  $\sigma$  of the host galaxy in such objects cannot be measured reliably because the light from the galaxy is overwhelmed by the quasar flux; instead, they use the width of the narrow [O III] emission line as a surrogate for  $\sigma$ . They estimate the black-hole mass using the “photoionization” method, which is based on an empirically calibrated relation involving the continuum luminosity of the active galactic nucleus (AGN) and the width of the H $\beta$  or other broad emission lines. The theoretical assumptions that underlie this relation are that the bulk velocities of the emitting clouds are determined by their orbital motion in the gravitational field of the black hole, and that the emitting region is photoionized by an ultraviolet continuum spectrum of fixed shape. They find an  $M_{\bullet} - \sigma$  relation that is consistent with the local one, suggesting that this relation is independent of redshift.

---

<sup>1</sup>The National Optical Astronomy Observatory is operated by AURA, Inc., under cooperative agreement with the National Science Foundation.

- Using similar methods on a larger but lower-redshift quasar sample from the Sloan Digital Sky Survey, Salviander et al. (2006) find that galaxies of a given dispersion at  $z \simeq 1$  have black-hole masses that are larger by  $\Delta \log_{10} M_{\bullet} \sim 0.2$  than at  $z = 0$ .
- Treu et al. (2004) and Woo et al. (2006) measured the velocity dispersion of 14 Seyfert I galaxies at redshift  $z \simeq 0.36$ ; they used stellar absorption lines, which should provide a more direct measure of the dispersion than emission lines. They measured the black-hole mass using the photoionization method. They found that galaxies of a given dispersion at  $z \simeq 0.36$  host black holes having  $\Delta \log_{10} M_{\bullet} = 0.62 \pm 0.10 \pm 0.25$ .
- Peng et al. (2006) measured the bulge luminosities of 11 quasar hosts in the redshift range  $1.7 < z < 2.7$  using the Hubble Space Telescope (HST), and estimated their black-hole masses using the photoionization method. They conclude that the  $M_{\bullet} - L$  relation at  $z \sim 2$  is close to the relation at  $z = 0$ ;  $\Delta \log_{10} M_{\bullet} \simeq -0.1$ . This result is remarkable since black holes can only grow with time, while elliptical galaxies fade with time as their stars die: even if the black holes do not grow at all, passive stellar evolution models would predict  $\Delta \log_{10} M_{\bullet}$  between  $-0.4$  and  $-0.8$  at  $z \simeq 2$ . If their result is correct, then either black holes must be ejected from the galaxy centers and replaced with smaller ones, or the galaxy luminosity must grow substantially through mergers.

A common thread among all these investigations and others is that the high-redshift sample is selected by some measure of AGN visibility. Black-hole masses and galaxy properties are then derived and an  $M_{\bullet} - \sigma$  or  $M_{\bullet} - L$  relation is fitted to the data. Since the low-redshift relations are linear in  $\log_{10} M_{\bullet}$ ,  $\log_{10} L$ , and  $\log_{10} \sigma$  (eqs. 4 or 5 below), the high-redshift data are often analyzed by assuming that the slope of the relation is the same as at low redshift and estimating the offset in the intercept or zero-point, which may be expressed as  $\Delta \log_{10} M_{\bullet}$  at fixed  $L$  or  $\sigma$ . Any such offset is then interpreted as evidence that the ratio of  $M_{\bullet}$  to  $\sigma$  or  $L$  has changed over time. Of course, the offset can be (and sometimes is) equally well expressed as  $\Delta \log_{10} L$  or  $\Delta \log_{10} \sigma$  at fixed black-hole mass.

Proof of evolution in the  $M_{\bullet}$  relations requires demonstrating that the high- and low-redshift galaxy samples were assembled with no selection effects that would bias the relation between the typical galaxy properties and black-hole masses being measured—or, at least, that the selection effects in the high- and low-redshift samples were the same. This may be a more difficult task than has commonly been assumed. The local black-hole sample has mostly been drawn from “normal” galaxies with quiescent or low levels of nuclear activity. Despite the proximity of these galaxies, detecting and weighing their central black holes requires exquisite spatial resolution, very high signal-to-noise observations, and elaborate

modeling of the observations. Investigating the properties of black holes in nearby galaxies remains a frontier problem; to date, dynamically determined black-hole masses are available for only slightly more than three dozen galaxies. Since there was little evidence of a black hole in most of these galaxies before HST observations were taken (except sometimes for a modest rise in the velocity dispersion in spectra taken at ground-based resolution), and since black holes are found in almost all nearby galaxies that have been examined carefully with HST, the black holes in local quiescent galaxies are selected mainly on the basis of galaxy properties such as  $L$  or  $\sigma$ .

The techniques used to measure black-hole masses in quiescent galaxies at low redshift cannot be used at high redshift, both because the radius of influence of the black hole cannot be resolved beyond a few tens of Mpc, and because the galaxies have substantially lower surface brightness, by the factor  $(1+z)^4$ . Black holes at high redshift are identified instead by their association with AGN. The observer thus *first* locates a black hole that is accreting matter and weighs it by the properties of the AGN emission lines (a difficult task, but one that we shall not examine in detail here), and then *secondly* attempts the (still difficult) task of measuring the properties of the host galaxy. The existence and properties of the AGN depend both on the properties of the black hole (mass, spin, orientation) and on the properties of the galaxy (mass inflow rate, orientation, etc.). In short, selection is done at low redshift by galaxy properties, and at high redshift by a combination of black-hole and galaxy properties that depends on the method used.

Galaxy samples obtained with different selection techniques will generally satisfy different  $M_\bullet$  relations. This effect, analogous to the Malmquist (1924) bias that is familiar in studies of Galactic structure, arises because of the cosmic scatter in the  $M_\bullet$  relations—there is not (so far as we know) an exact 1–1 relation between black-hole mass and any single measurable property of galaxies such as  $L$  or  $\sigma$ . In this paper we argue that determinations of the redshift evolution of the  $M_\bullet$  relations may be strongly biased by selection effects unless the same sample selection techniques are used at all redshifts. Correcting for the selection bias introduced by the use of different sample selection criteria at different redshifts is extremely difficult: to make accurate corrections it is necessary to know both how the selection depends on the galaxy and black-hole properties and the cosmic scatter in the  $M_\bullet$  relations. At present we have only crude upper limits to the latter quantity. We shall show that even if the cosmic scatter were known, the bias in the samples described above usually can only be corrected with additional information, such as how galaxy properties and black-hole mass determine the probability distribution of AGN luminosity.

The selection bias can be especially large at large  $M_\bullet$ , as the following argument shows. Consider the  $M_\bullet - L$  relation. At high  $L$  the number density of galaxies falls off rapidly, as

illustrated by the steep cutoff in the Schechter (1976) luminosity function. Cosmic scatter in the  $M_{\bullet} - L$  relation implies that there is a distribution of black-hole masses at a given  $L$ . The rare high-mass black holes can arise from either the peak of this distribution in the rare galaxies with large  $L$ , or from the high-mass tail of the distribution in the more numerous galaxies of modest  $L$ . If the number density of galaxies is falling off rapidly with  $L$ , the contribution from galaxies with modest  $L$  may actually overwhelm the population of black holes of similar mass associated with galaxies of higher  $L$ . This problem was first explicitly identified by Fine et al. (2006) in the context of the correlation between black-hole mass and dark-matter halo mass, and by Salviander et al. (2006) in the context of the  $M_{\bullet} - \sigma$  relation, but apparently has not been appreciated by most observers studying the evolution of the  $M_{\bullet}$  relations.

In this paper we present a more general exposition of the biases incurred when studying evolution of the  $M_{\bullet}$  relations by comparing samples obtained by different selection criteria and at different redshifts. We start by considering the extraction of samples from hypothetical joint distributions of  $M_{\bullet}$  and  $L$  or  $\sigma$ . We then consider the selection bias that occurs if the high-redshift samples are selected by AGN flux or luminosity. We discuss the prospects of correcting for selection bias, and argue that selection bias may place fundamental limits on the determination of the evolution of the  $M_{\bullet}$  relations. We conclude with a brief review of attempts to measure the evolution of the  $M_{\bullet}$  relations and how they may have been affected by selection bias.

## 2. The Joint Distribution of Black-Hole Mass and Galaxy Properties

Understanding object selection bias requires knowledge of the joint probability distribution of black-hole mass  $M_{\bullet}$  and a galaxy property  $s$ , which for the present discussion is either  $\log_{10} L$ , where  $L$  is the rest-frame  $V$ -band galaxy luminosity, or  $\log_{10} \sigma$ , where  $\sigma$  is the line-of-sight velocity dispersion in the main body of the galaxy (the precise definition of  $L$  or  $\sigma$  does not concern us, so long as it is defined consistently in all samples). The true form of the joint distribution unfortunately is unknown; however, we can construct a hypothetical form of this distribution that accurately represents the present state of the observations, and in any case suffices to show how sample selection bias can occur.

We write the probability of finding a galaxy in the interval  $(\mu, \mu + d\mu)$  and  $(s, s + ds)$  as  $\nu(\mu, s) d\mu ds$  where  $\mu = \log_{10}(M_{\bullet})$ . From the definition of conditional probability this can be rewritten as

$$\nu(\mu, s) = \nu(\mu|s)g(s), \tag{1}$$

where  $g(s) ds$  is the probability that a randomly chosen galaxy in a given volume lies in the

interval  $(s, s + ds)$  and  $\nu(\mu|s) d\mu$  is the probability that the black-hole mass lies in the range  $(\mu, \mu + d\mu)$  given that the galaxy property is  $s$ . The function  $g(s)$  is then given by either the volume-limited luminosity function—more properly, the luminosity function of early-type galaxy components (ellipticals and spiral bulges), since these are the components that correlate with black-hole mass—or the velocity-dispersion distribution of early-type components. Without loss of generality, we may write  $\nu(\mu, s) = h[\mu - f(s), s]$  where  $\int h(x, y) dx = 1$  and  $\int xh(x, s) dx = 0$ , so  $f(s)$  is the mean value of  $\mu$  at a given value of the galaxy property  $s$ —that is,  $f(s)$  is either the  $M_{\bullet} - L$  or  $M_{\bullet} - \sigma$  relation. The limited observational data on black-hole masses in local galaxies is consistent with the hypothesis that  $h(x, s)$  is independent of  $s$ ; adopting this hypothesis for simplicity we have

$$\nu(\mu, s) = h[\mu - f(s)] g(s). \quad (2)$$

The intrinsic variance or “cosmic scatter” in black-hole mass at a given value of galaxy property  $s$  is  $\sigma_{\mu}^2 = \int x^2 h(x, s) dx$ . Observational errors may make  $h(x, s)$  appear to be yet broader, but for this discussion, we assume that observational errors are negligible; the selection effects that we are concerned with are solely due to the fact that there is an intrinsic and irreducible range of  $M_{\bullet}$  at any  $s$ .

It should be stressed that although the functional form (2) is consistent with the available data, it is far from unique. As a foil, we may consider the form

$$\nu(\mu, s) = p[s - c(\mu)] \Phi_{\bullet}(\mu). \quad (3)$$

A physical model that motivates (2) is one in which the galaxy property  $s$  determines the black-hole mass  $\mu$  with a cosmic scatter described by the function  $h$ , while (3) is motivated by models in which the black-hole mass  $\mu$  determines the galaxy property  $s$ , with cosmic scatter described by the function  $p$ . If  $\int p(y) dy = 1$ , then  $\Phi_{\bullet}(\mu) d\mu$  is the number of black holes per unit volume with log mass in the range  $(\mu, \mu + d\mu)$ . We do not know which of (2) or (3) is correct (possibly neither, or both); our motivation for choosing the former is that it provides a simple representation of what local observations of black holes in inactive galaxies measure.

Of the three functions that contribute to  $\nu(\mu, s)$ ,  $g(s)$  is probably the best determined. We discuss the galaxy-property functions in detail in Lauer et al. (2007), but summarize them briefly here. For the galaxy luminosity function we use the Blanton et al. (2003) Sloan Digital Sky Survey (SDSS) luminosity function, transformed to the  $V$ -band and redshift  $z = 0.1$ , augmented with the Postman & Lauer (1995) luminosity function of brightest cluster galaxies, which appear to be undercounted in the SDSS. We note that the Blanton et al. function refers to total rather than bulge luminosity in S0 and spiral galaxies; however, this difference is less important at the bright end of the luminosity function, where the

selection effects are strongest. For the velocity-dispersion function we use the Sheth et al. (2003) SDSS results, augmented at the high- $\sigma$  end as prescribed by Bernardi et al. (2006) to account for an artificial high- $\sigma$  cut-off in Sheth et al. Both functions are shown in Figure 1.

The function  $f(s)$  should be the least-squares fit of  $\log_{10} M_{\bullet}$  to  $\log_{10} L$  or  $\log_{10} \sigma$  in a sample selected by galaxy properties. The  $M_{\bullet} - \sigma$  relation  $f(s)$  is based on the galaxy sample from Tremaine et al. (2002) augmented by a few galaxies with more recent  $M_{\bullet}$  determinations (see Lauer et al. 2007). In contrast to the treatment in Tremaine et al. (2002), which treated  $M_{\bullet}$  and  $\sigma$  symmetrically, the appropriate treatment for our purposes is a least-squares fit of  $\log_{10} M_{\bullet}$  on  $\log_{10} \sigma$ , which gives:

$$\log_{10}(M_{\bullet}/M_{\odot}) = (4.13 \pm 0.32) \log_{10}(\sigma/200 \text{ km s}^{-1}) + 8.29 \pm 0.07, \quad (4)$$

for  $H_0 = 70 \text{ km s}^{-1} \text{ Mpc}^{-1}$  (which we will use throughout this paper). We discuss the  $M_{\bullet} - L$  relation in detail in Lauer et al. (2007); in brief we use the Häring & Rix (2004) relation between  $M_{\bullet}$  and galaxy *mass*, transformed back to luminosity by adopting the mass-to-light ratio  $M/L_V \simeq 6 \times 10^{-0.092(M_V+22)} M_{\odot}/L_{\odot}$ , based on the  $M/L$  estimates given in Gebhardt et al. (2003). A least-squares fit of  $M_{\bullet}$  on  $M_V$  for galaxies with  $M_V < -19$  gives:

$$\log_{10}(M_{\bullet}/M_{\odot}) = (1.32 \pm 0.14)(-M_V - 22)/2.5 + 8.67 \pm 0.09. \quad (5)$$

Equations (4) and (5) have the form

$$f(s) = a + bs, \quad (6)$$

where  $a$  and  $b$  are constants. Lauer et al. (2007) show that the  $M_{\bullet} - \sigma$  and  $M_{\bullet} - L$  relations make different predictions for  $M_{\bullet}$  in luminous or high-dispersion galaxies, which have lower  $\sigma$  values for a given luminosity than is implied by eliminating  $M_{\bullet}$  from equations (4) and (5). Thus at least one of the  $M_{\bullet} - \sigma$  or  $M_{\bullet} - L$  relations must curve away from the linear fit (6) in the most luminous galaxies. We are not concerned with this issue here, and simply show the different selection biases that can result from using  $\sigma$  or  $L$  as the galaxy property that correlates with  $M_{\bullet}$ , *assuming* that the linear relation (6) holds at all masses. However, the reader should bear in mind that neither the  $M_{\bullet} - L$  or  $M_{\bullet} - \sigma$  relation is well determined at high galaxy masses, where the potential selection bias is most important.

The scatter function,  $h[\mu - f(s)]$ , is poorly known at best. For this analysis, we assume that at any galaxy  $L$  or  $\sigma$ ,  $\log_{10} M_{\bullet}$  is described by a normal distribution about  $f(s)$ , with cosmic scatter  $\sigma_{\mu}$ . Thus

$$h[\mu - f(s)] d\mu = \frac{d\mu}{\sqrt{2\pi\sigma_{\mu}^2}} \exp\left[-\frac{[\mu - f(s)]^2}{2\sigma_{\mu}^2}\right]. \quad (7)$$

Again, we emphasize that  $\sigma_\mu$  does not embody any observational errors in the determination of  $M_\bullet$ ; it represents the intrinsic spread in  $M_\bullet$  at any galaxy property. Novak et al. (2006) conclude that only an upper limit to  $\sigma_\mu$  is presently known for either the  $M_\bullet - \sigma$  or  $M_\bullet - L$  relation, both because of the small sample of reliable  $M_\bullet$  determinations, and because of uncertainties in the observational errors in  $M_\bullet$ , which must be accurately measured to isolate the contribution of  $\sigma_\mu$  to the total residuals. For the present analysis we will explore the sensitivity of the selection biases to  $\sigma_\mu$  on the assumption that  $\sigma_\mu < 0.3$  for dispersion  $\sigma$  and  $\sigma_\mu < 0.5$  for luminosity  $L$ .

Apart from the poor knowledge of  $\sigma_\mu$ , there are at least two other major uncertainties in the function  $h$ : (i) a more general treatment would allow for the possibility that it varies with  $s$ ; (ii) there is little or no justification of the assumed normal form. As will be shown below, for the most massive black holes or galaxies, the selection bias may depend on the form that  $h[\mu - f(s)]$  takes at several standard deviations away from the mean, yet an observational determination of the form of  $h$  in this region would require a sample of well-determined black-hole masses several orders of magnitude larger than is presently available. Thus at the highest black-hole masses, the selection bias is likely to depend sensitively on knowledge that is not presently at hand, so it is not possible to apply reliable corrections for this bias.

With these caveats, in Figure 2 we show estimates of  $\nu(\mu, s)$  as modeled by equation (2) for each of the  $M_\bullet - \sigma$  and  $M_\bullet - L$  relations, and two assumed values of  $\sigma_\mu$ . Projection of  $\nu(\mu, s)$  onto the  $\mu$ -axis produces the mass function of black holes,

$$\Phi_\bullet(\mu) = \int \nu(\mu, s) ds \quad (8)$$

$$= \int h[\mu - f(s)] g(s) ds. \quad (9)$$

The importance of cosmic scatter for converting the luminosity or dispersion function  $g(s)$  to a black-hole mass function has been discussed several times (Yu & Tremaine 2002; Yu & Lu 2004; Tundo et al. 2006; Lauer et al. 2007). What may be less appreciated, however, is that cosmic scatter implies that the most massive BHs are often hosted by modest galaxies that *a priori* would not be expected to harbor BHs of high mass. To illustrate this point, Figure 3 shows  $\Phi_\bullet(\mu)$  for four different versions of  $\nu(\mu, s)$ . The salient feature is that as the cosmic scatter  $\sigma_\mu$  increases, the contribution to the density of the most massive black holes from the wings of the scatter function  $h$  overwhelms the “native” population of massive black holes harbored by the galaxies with the largest values of property  $s$ . A second illustration of this point occurs in the top two panels in Figure 4, which show the probability distribution of  $L$  and  $\sigma$  for  $M_\bullet = 10^{10} M_\odot$ : note that the solid curves, corresponding to  $\sigma_\mu = 0.5$  for  $L$  and 0.3 for  $\sigma$ , have a prominent shoulder to the right of the peak, the peak arising from low-luminosity or low-dispersion galaxies, and the shoulder from high luminosities and dispersions.

The source of the selection bias can be seen more directly in Figure 2, which shows  $\nu(\mu, s)$  for each of the  $M_\bullet - \sigma$  and  $M_\bullet - L$  relations, and two assumed values of  $\sigma_\mu$ . Only for  $\sigma_\mu = 0$  is there an exact relation between  $M_\bullet$  and  $\sigma$  or  $L$ . Our model for  $\nu(\mu, s)$ —which may not be correct, but is consistent with the data—implies that the density contours in Figure 2 are symmetric about the mean relationship ridge-lines in the vertical direction; in other words, the conditional probability of  $\mu$  given  $s$  is symmetric about  $\mu = f(s)$ . On the other hand, the conditional probability of  $s$  given  $\mu$ ,

$$\nu(s|\mu) = \frac{\nu(\mu, s)}{\int \nu(\mu, s) ds}, \quad (10)$$

is not symmetric about  $s = f^{-1}(\mu)$ , as seen in Figure 4, which shows the distribution of  $s$  at selected values of  $M_\bullet$ . As  $M_\bullet$  and  $\sigma_\mu$  increase, the distribution of  $s$  for a given  $M_\bullet$  moves further and further away from the value implied by the inverse of the  $M_\bullet$  relations,  $f^{-1}(\mu) = (\mu - a)/b$ , where  $a$  and  $b$  are the coefficients given in equation (6). For  $M_\bullet > 10^9 M_\odot$ ,  $f^{-1}(\mu)$  generally falls well out in the wings of the distribution of  $s$  for both  $L$  and  $\sigma$ , particularly for the larger values of  $\sigma_\mu$ . The galaxies with  $s = f^{-1}(\mu)$  for the highest mass black holes are so far down in the step cutoffs of the  $L$  and  $\sigma$  distribution functions that they are completely overwhelmed by the population of galaxies of modest mass that harbor high mass black holes as statistical outliers.

The mean value of  $s$  at a given  $M_\bullet$  is

$$\langle s \rangle_\mu = \int s \nu(s|\mu) ds = \frac{\int s \nu(\mu, s) ds}{\int \nu(\mu, s) ds} = \frac{\int s g(s) h[\mu - f(s)] ds}{\int g(s) h[\mu - f(s)] ds}. \quad (11)$$

This is shown as the red lines in Figure 2. The mean of  $\log_{10} L$  or  $\log_{10} \sigma$  at a given  $M_\bullet$  is offset from  $f^{-1}(\mu)$ , which is just the  $s$  location of the  $M_\bullet$  relation ridgelines shown in the Figure. In the presence of cosmic scatter, the mean  $s$  of a sample of galaxies that host a black hole of given  $\mu$  is different from the mean  $\mu$  hosted by a sample of galaxies of given  $s$ . This difference is the source of the selection bias.

### 3. Illustration of Selection Biases

Selection bias typically occurs because the galaxy samples used to probe the  $M_\bullet$  relations at cosmological distances are not selected by galaxy  $L$  or  $\sigma$ , but by the visibility of their AGNs. For most of the discussion in this section we shall assume that AGN luminosity does not depend directly on  $L$ ,  $\sigma$ , or any other galaxy property unrelated to  $M_\bullet$ . This model is appropriate if, for example, the probability that the AGN associated with a black hole of

mass  $M_\bullet$  has luminosity  $L_{\text{AGN}}$  is given by

$$dp = \psi(\lambda - \mu) d\lambda \quad \text{where} \quad \int \psi(x) dx = 1 \quad (12)$$

and  $\lambda \equiv \log_{10} L_{\text{AGN}}$  and  $\mu = \log_{10} M_\bullet$ . The physical content of this assumption is that the luminosity history of an AGN is determined by the black-hole mass and scales with the Eddington luminosity, which is proportional to  $M_\bullet$ .

### 3.1. Bias in a Luminosity-Limited Survey

We first consider the bias that occurs in a sample in which (i) all of the objects are in a narrow redshift range; (ii) the survey contains all AGNs brighter than a given flux. In this case the probability that an AGN in the relevant redshift range is accepted in the survey depends only on its luminosity  $L_{\text{AGN}}$ , and by equation (12) this in turn depends only on its black-hole mass  $\mu$ . Thus the probability distribution of a galaxy property  $s$  at a given value of  $\mu$  is not biased by the selection, and is simply  $\nu(s|\mu)$  (eq. 10). Some examples are shown in Figure 4, which plots the probability distribution of  $s - f^{-1}(\mu)$  for several values of black-hole mass  $M_\bullet$  and cosmic scatter  $\sigma_\mu$ . Here  $f^{-1}(s)$  is the inverse of the  $M_\bullet - L$  or  $M_\bullet - \sigma$  relation (eq. 2). The mean values of the distributions  $\langle s \rangle_\mu$  are displaced to values lower than  $f^{-1}(\mu)$  in most of the examples shown. As expected, the width and offset of the distributions are larger for larger values of  $\sigma_\mu$ . Also as expected, the offsets are generally larger for more massive black holes.  $\langle s \rangle_\mu$  is shown as the red lines in Figure 2; the offset of these lines from the relation  $\mu = f(s)$  demonstrates the selection bias.

In this model, the selection bias can be corrected: an assumed form for the probability distribution  $\nu(\mu, s)$  such as (2) with redshift-dependent parameters can be used to compute  $\nu(s|\mu)$ , which can then be fitted to the distribution of galaxy property  $s$  in the sample at a given value of black-hole mass  $\mu$  (separate issues, discussed in §4, are whether this model for the selection effects is realistic and whether the assumed form of  $\nu(\mu, s)$  is correct). However, most papers in the literature have not taken this approach, so it is worthwhile to estimate the biases that might be introduced by using simpler statistics to estimate the evolution in the  $M_\bullet$  relations.

Figure 5 shows the object selection bias  $\Delta s = f^{-1}(\mu) - \langle s \rangle_\mu$  as a function of  $M_\bullet$  and  $\sigma_\mu$ . In this example we have expressed the bias in terms of galaxy properties, since we have selected by  $M_\bullet$ ; however, it may also be represented as  $\Delta \log_{10} M_\bullet = b \Delta s$ , where  $b$  is the slope given in equation (6). Note that the bias is not always a monotonic function of black-hole mass, nor does it always have the same sign. In this simple model, the bias at black-hole masses of  $10^9 M_\odot$  is  $\Delta \log_{10} M_\bullet = 0.4$  in the  $M_\bullet - \sigma$  relation for  $\sigma_\mu = 0.3$ , and

$\Delta \log_{10} M_{\bullet} = 0.7$  in the  $M_{\bullet} - L$  relation for  $\sigma_{\mu} = 0.5$ —and even larger at larger black-hole masses. The bias is smaller at lower  $L$  or  $\sigma$ , but we caution that the near-zero bias in the  $M_{\bullet} - L$  relation at small  $M_{\bullet}$  is an artifact of our assumption that the luminosity function has the Schechter (1976) form at low luminosities (see below), and this may not be true for the early-type galaxy components that are believed to host the black holes.

Figure 5 also shows that a significant portion of the bias comes from galaxies with  $|s - f^{-1}(\mu)| > 2\sigma_{\mu}$  for the larger values of  $\sigma_{\mu}$ . Indeed for  $M_{\bullet} \approx 5 \times 10^9 M_{\odot}$ , nearly half of the bias comes from such galaxies for all but the smallest  $\sigma_{\mu}$  shown. Thus, not only is the bias sensitive to  $\sigma_{\mu}$ , it also depends on the shape of the wings of the error distribution. If, as is likely, the wings are more extended than in our assumed log-normal distribution, the bias will be even larger.

Many of the features in these plots can be understood analytically. From the definition of  $\langle s \rangle_{\mu}$  (equation 11) and equation (6), we can write

$$a + b\langle s \rangle_{\mu} = \mu - \frac{\int x h(x) g[b^{-1}(\mu - a - x)] dx}{\int h(x) g[b^{-1}(\mu - a - x)] dx}. \quad (13)$$

If the cosmic scatter  $\sigma_{\mu}^2 = \int dx x^2 h(x)$  is not too large, we can evaluate this by expanding  $g(s)$  in a Taylor series,

$$a + b\langle s \rangle_{\mu} = \mu + \sigma_{\mu}^2 \left[ \frac{d \ln g(s)}{ds} \right]_{s=(\mu-a)/b} + \mathcal{O}(\sigma_{\mu}^4). \quad (14)$$

This result shows that (i) the bias is proportional to  $\sigma_{\mu}^2$  if  $\sigma_{\mu}$  is not too large; (ii) the bias in  $\langle s \rangle_{\mu}$  is positive if  $g(s)$  declines with  $s$  and proportional to  $d \ln g(s)/ds$ —this is why the bias is large and negative for the most luminous or high-dispersion galaxies; (iii) the bias is near zero if  $g(s)$  is constant, which corresponds to a luminosity function  $dn \propto dL/L$  when  $s = \log_{10} L$ . The bias in the left panel of Figure 5 is small for low-luminosity galaxies because the assumed luminosity function is close to this form.

A different statistical method, which more closely parallels the approach used in most observational papers, is simply to estimate the average value of the difference between  $\mu$  and the prediction of the  $\mu - s$  relation (6) for all the galaxies in the sample,

$$\Delta \log_{10} M_{\bullet} \equiv \langle \mu - f(s) \rangle = \langle \mu \rangle - a - b\langle s \rangle, \quad (15)$$

Let us assume that the survey flux limit at the given redshift corresponds to a luminosity  $L_0$  with  $\lambda_0 = \log_{10} L_0$ . Then

$$\Delta \log_{10} M_{\bullet} = \frac{\int_{\lambda_0}^{\infty} d\lambda \int g(s) ds \int (\mu - a - bs) h(\mu - a - bs) \psi(\lambda - \mu) d\mu}{\int_{\lambda_0}^{\infty} d\lambda \int g(s) ds \int h(\mu - a - bs) \psi(\lambda - \mu) d\mu} \quad (16)$$

$$= \frac{\int_{\lambda_0}^{\infty} d\lambda \int g(s) ds \int x h(x) \psi(\lambda - x - a - bs) dx}{\int_{\lambda_0}^{\infty} d\lambda \int g(s) ds \int h(x) \psi(\lambda - x - a - bs) dx} \quad (17)$$

$$= \frac{\int_{\lambda_0}^{\infty} d\lambda \int x h(x) \phi(\lambda - x) dx}{\int_{\lambda_0}^{\infty} d\lambda \int h(x) \phi(\lambda - x) dx}, \quad (18)$$

where  $x \equiv \mu - a - bs$ , and

$$\phi(y) = \int g(s) \psi(y - a - bs) ds. \quad (19)$$

The luminosity function (number per unit volume) of AGNs is  $dn = \Psi(\lambda)d\lambda$ , where

$$\Psi(\lambda) = \int g(s) ds \int h(\mu - a - bs) \psi(\lambda - \mu) d\mu = \int h(x) \phi(\lambda - x) dx, \quad (20)$$

which is just the inner integral of the denominator of (18). To evaluate the inner integral in the numerator of equation (18), note that the functional form of  $h(x)$  (eq. 7) implies that  $h'(x) = -xh(x)/\sigma_\mu^2$ , so

$$\int x h(x) \phi(\lambda - x) dx = -\sigma_\mu^2 \int h'(x) \phi(\lambda - x) dx. \quad (21)$$

Integrating the right side of the equation by parts, and noting that  $\lim_{y \rightarrow \infty} \phi(y) = 0$ , gives

$$\int x h(x) \phi(\lambda - x) dx = \sigma_\mu^2 \int h(x) \frac{\partial}{\partial x} \phi(\lambda - x) dx \quad (22)$$

$$= -\sigma_\mu^2 \int h(x) \frac{\partial}{\partial \lambda} \phi(\lambda - x) dx \quad (23)$$

$$= -\sigma_\mu^2 \frac{d}{d\lambda} \int h(x) \phi(\lambda - x) dx. \quad (24)$$

Thus

$$\Delta \log_{10} M_\bullet = \frac{\sigma_\mu^2 \Psi(\lambda_0)}{\int_{\lambda_0}^{\infty} \Psi(\lambda) d\lambda}. \quad (25)$$

Remarkably, the result depends only on the directly observable luminosity function  $\Psi(\lambda)$  for the type of AGN targeted in the survey, and is independent of assumptions about the luminosity history  $\psi(\lambda - \mu)$  or the distribution of host galaxy properties  $g(s)$ . Also, in contrast to the analogous result (14), equation (25) is not just the first term in a Taylor series in  $\sigma_\mu^2$  but valid for all values of  $\sigma_\mu^2$ , no matter how large.

To illustrate the application of this result, we adopt the quasar luminosity function from Boyle et al. (2003),

$$\Psi(\lambda) = \frac{\Psi_*}{10^{-(1+\alpha)(\lambda-\lambda^*)} + 10^{-(1+\beta)(\lambda-\lambda^*)}}, \quad (26)$$

with  $\alpha = -3.4$  and  $\beta = -1.6$ , where  $\lambda^*$  is the “break” luminosity. The corresponding bias  $\Delta \log_{10} M_{\bullet}$  is shown as a function of the lower luminosity limit  $\lambda_0 - \lambda^*$  in Figure 6. Note that the bias in Figure 6 becomes smaller but does not vanish as the survey goes to fainter and fainter luminosity limits: asymptotically,  $\Delta \log_{10} M_{\bullet} \rightarrow -(1 + \beta) \ln 10$  which equals  $0.12(\sigma_{\mu}/0.3)^2$ .

### 3.2. Bias in a Flux-Limited Survey

As a second example, we examine the bias in a flux-limited sample of AGN. We assume that the survey galaxies are distributed uniformly in Euclidean space, that the probability distribution of AGN luminosities is given by equation (12), and that the survey contains all galaxies with flux  $f = L_{\text{AGN}}/r^2$  exceeding some limiting flux  $f_0$ .

The bias is then given by

$$\Delta \log_{10} M_{\bullet} = \frac{\int d\lambda \int g(s) n V(\lambda) ds \int (\mu - a - bs) h(\mu - a - bs) \psi(\lambda - \mu) d\mu}{\int d\lambda \int g(s) n V(\lambda) ds \int h(\mu - a - bs) \psi(\lambda - \mu) d\mu}, \quad (27)$$

where  $V(\lambda) = \frac{1}{3} \Delta \Omega (L_{\text{AGN}}/f_0)^{3/2} \propto 10^{3\lambda/2}$  is the volume within which an AGN of luminosity  $\lambda$  can be detected,  $\Delta \Omega$  is the solid angle covered by the survey, and  $n$  is the number density of galaxies. We have

$$\Delta \log_{10} M_{\bullet} = \frac{\int d\lambda \int g(s) 10^{3\lambda/2} ds \int (\mu - a - bs) h(\mu - a - bs) \psi(\lambda - \mu) d\mu}{\int d\lambda \int g(s) 10^{3\lambda/2} ds \int h(\mu - a - bs) \psi(\lambda - \mu) d\mu} \quad (28)$$

$$= \frac{\int 10^{3\lambda/2} d\lambda \int g(s) ds \int x h(x) \psi(\lambda - x - a - bs) dx}{\int 10^{3\lambda/2} d\lambda \int g(s) \int h(x) \psi(\lambda - x - a - bs) dx} \quad (29)$$

$$= \frac{\int 10^{3\lambda/2} d\lambda \int x h(x) \phi(\lambda - x) dx}{\int 10^{3\lambda/2} d\lambda \int h(x) \phi(\lambda - x) dx}, \quad (30)$$

where  $\phi(y)$  is defined by equation (19). To evaluate the inner integral in the numerator of equation (30) we use equation (24), which yields

$$\Delta \log_{10} M_{\bullet} = -\sigma_{\mu}^2 \frac{\int 10^{3\lambda/2} d\lambda \frac{d}{d\lambda} \int h(x) \phi(\lambda - x) dx}{\int 10^{3\lambda/2} d\lambda \int h(x) \phi(\lambda - x) dx} \quad (31)$$

$$= \frac{3 \ln 10}{2} \sigma_{\mu}^2, \quad (32)$$

where the last line follows from an integration of the numerator by parts.

### 3.3. Selection Effects That Depend Only on Galaxy Properties

The results of the previous subsections depend on the assumption that the probability distribution of AGN luminosity is determined by the black-hole mass and not the galaxy properties (eq. 12). A foil to this is to assume that the luminosity is determined by the galaxy properties and not the black-hole mass. Thus equation (12) is replaced by

$$dp = \chi(\lambda - ks) d\lambda \quad \text{where} \quad \int \chi(x) dx = 1 \quad (33)$$

where  $k$  is a constant. In this case  $\Delta \log_{10} M_{\bullet} = 0$  in any flux-limited or luminosity-limited sample (Salviander et al. 2006).

## 4. Correcting for Selection Bias May be Extremely Difficult

Given the example bias calculations shown in the previous section, it may be tempting to conclude that similar bias corrections may be estimated and applied after the fact to existing surveys to determine the  $M_{\bullet} - \sigma$  or  $M_{\bullet} - L$  relations. We believe that in general such corrections are difficult or impossible to apply reliably to current surveys, for the following reasons.

### 4.1. The Error Model is Poorly Known

In the examples above, we assumed that at any galaxy property  $s$ ,  $\mu = \log_{10} M_{\bullet}$  followed a normal distribution about the mean  $M_{\bullet} - s$  relation  $\mu = f(s)$ , with standard deviation characterized by a cosmic scatter  $\sigma_{\mu}$ . We saw that the bias is very sensitive to  $\sigma_{\mu}$  (in most examples  $\propto \sigma_{\mu}^2$ ) yet this parameter is poorly known for either the  $M_{\bullet} - \sigma$  or  $M_{\bullet} - L$  relations, in part because an accurate estimate of  $\sigma_{\mu}$  requires knowing the observational errors in the  $M_{\bullet}$  determinations. Novak et al. (2006) have studied this problem and conclude only that  $\sigma_{\mu} \lesssim 0.3$  for the  $M_{\bullet} - \sigma$  relation and  $\sigma_{\mu} \lesssim 0.5$  for the  $M_{\bullet} - L$  relation. Moreover, the Novak et al. (2006) analysis assumes, as we do, that  $\sigma_{\mu}$  is constant over the parameter range of the  $M_{\bullet}$  relations; the sample of galaxies with well-determined  $M_{\bullet}$  is simply too small to explore the possibility that it is not.

Even if an accurate estimate of  $\sigma_{\mu}$  were available, the functional form of the distribution of  $\mu - f(s)$  is unknown. The assumption of a normal distribution is an obvious first step, yet the steep falloff of the  $L$  or  $\sigma$  distribution at large values means that the selection bias for large black-hole masses is sensitive to the wings of this distribution, where  $\mu - f(s) \gtrsim 2\sigma_{\mu}$ .

The assumed normal distribution is likely to *underestimate* the selection bias since more realistic distributions have fatter tails. Given that the local black-hole sample is so small that  $\sigma_\mu$  is poorly determined, the sample of galaxies with good  $M_\bullet$  determinations would have to be several orders of magnitudes larger before an accurate form for the scatter function could be determined.

#### 4.2. The $M_\bullet$ Relationships are Poorly Known

The  $M_\bullet$  relations are imperfectly known at  $z = 0$ , and in particular the range of  $L$  or  $\sigma$  that is used to determine them is rather limited. For example, in the sample of 31 local galaxies with measured black-hole masses used by Tremaine et al. (2002) to determine the  $M_\bullet - \sigma$  relation, the interquartile ranges in  $L$  and  $\sigma$  are only factors of 5.3 and 1.6 respectively. Thus, the calculation of the selection biases for  $M_\bullet \gtrsim 10^9 M_\odot$  must contend with the fact that there are only a few black holes observed in this mass range in the local sample (4 in the Tremaine et al. 2002 sample). Lauer et al. (2007) show that the  $L - \sigma$  relation must be curved (in logarithmic coordinates) in the sense that  $\sigma$  appears to increase only slowly (if at all) with  $L$  for the most luminous galaxies. This implies that the present log-linear  $M_\bullet - \sigma$  and  $M_\bullet - L$  relation cannot be consistent at high galaxy luminosity. The joint  $M_\bullet - s$  distributions shown in Figure 2 are thus based on extrapolated estimates at the highest  $M_\bullet$  values that are likely to change if more and better determinations of black-hole masses  $M_\bullet \gtrsim 10^9 M_\odot$  become available.

#### 4.3. What Determines AGN Luminosity?

The heart of our analysis of selection bias in §§3.1 and 3.2 is the assumption that the black hole determines the AGN luminosity, or more precisely that the galaxy properties do not. This is clearly true if, for example, (i) black holes radiate either at the Eddington luminosity  $L_{\text{Edd}}$  or not at all, and (ii) the bolometric correction is independent of galaxy properties. This assumption is also true in more general circumstances, for example, (i) can be replaced by the weaker assumption that the probability that a black hole is radiating at some  $L_{\text{AGN}}$  depends only on the ratio  $L_{\text{AGN}}/L_{\text{Edd}}$  (eq. 12). This assumption may be approximately correct: for example, Hopkins et al. (2006) find that their simulations are well-fit by a model in which the probability distribution of AGN luminosities depends only on  $L_{\text{AGN}}/L_{\text{peak}}$  where  $L_{\text{peak}}$  is the peak luminosity of the AGN and  $L_{\text{peak}} \propto L_{\text{Edd}}^{1.12}$ . Nevertheless, if galaxy properties do affect the AGN luminosity—most likely by determining the feeding rate of matter onto the black hole at luminosities  $L \ll L_{\text{Edd}}$ —then the biases will be different

from those presented in §§3.1 and 3.2. In the limiting case that the AGN luminosity is determined entirely by galaxy properties rather than black-hole mass, as might be plausible for low-luminosity AGNs, there is no selection bias in a flux- or luminosity-limited survey (§3.3).

#### 4.4. Did the Galaxy Make the Black Hole, or the Black Hole the Galaxy?

We have assumed that the joint probability distribution of black-hole mass  $\mu$  and galaxy property  $s$  can be modeled by equation (2). This corresponds to a physical model in which the galaxy property is the independent variable, and the black-hole mass is determined by the properties of the galaxy through the cosmic-scatter function  $h(y)$  and the  $M_{\bullet}$  relation  $f(s)$ . This assumption is convenient for modeling the local sample of galaxies with  $M_{\bullet}$  determinations, which was selected by galaxy properties, plus the ready knowledge of  $g(s)$ , the volume distribution of  $s$ . The alternative model provided by equation (3), in which the black-hole mass is the independent variable and the galaxy property is determined by the black hole through the function  $p(y)$ , is much more difficult to fit to the local observations as we have little direct knowledge of  $\Phi_{\bullet}(\mu)$ , the black-hole mass function. However, our present understanding of black-hole and galaxy formation does not allow us to say which model, if either, is correct.

#### 4.5. Survey Selection Effects May be Poorly Known

Most of our estimates of selection bias have been based on the assumption that surveys are complete to a given AGN luminosity or flux, but this is an oversimplification. Any survey that is based on measurements of the luminosity of the host galaxy requires that the host is bright enough and large enough to be separated from the AGN. Any survey that uses the velocity dispersion measured from stellar absorption lines requires that the absorption lines are strong enough, and that AGN emission lines in the vicinity of the absorption lines are weak enough, to allow a reliable dispersion measurement. At the opposite extreme, surveys of low-luminosity AGNs require that the emission lines are strong enough to be detected against the continuum flux from the galaxy. In such studies the selection depends in a complex way on properties such as the ratio of AGN to galaxy luminosity, and on galaxy properties other than  $L$  or  $\sigma$ , such as the effective radius or central surface brightness.

## 5. Bias in Existing Surveys

We have intended this paper mainly as a planning guide for future surveys to explore the evolution of the  $M_{\bullet}$  relation, rather than as a critique of existing surveys. The following brief comments on existing surveys are mostly intended to illustrate the application and impact of the estimates of selection bias that we have made in earlier sections.

Several authors have determined the  $M_{\bullet} - \sigma$  relation for nearby AGNs, and compared this to the local relation for inactive galaxies. Using seven Seyfert 1 galaxies with black-hole masses measured by reverberation mapping, Gebhardt et al. (2000b) find  $\Delta \log_{10} M_{\bullet} = -0.21 \pm 0.13$ . For 16 AGNs with reverberation-based black-hole masses Onken et al. (2004) find  $\Delta \log_{10} M_{\bullet} = -0.26 \pm 0.15$  (although Onken et al. interpret their result in terms of calibrating the reverberation-mapping method rather than an offset in the  $M_{\bullet} - \sigma$  relation). Barth, Greene, & Ho (2005) have compared the black-hole masses in dwarf Seyfert 1 galaxies to an extrapolation of the  $M_{\bullet} - \sigma$  relation to lower dispersions; using black-hole masses based on the photoionization method calibrated by the standard “isotropic” formula, they find  $\Delta \log_{10} M_{\bullet} = -0.04$  (although they interpret their results with Onken et al.’s calibration and thus find  $\Delta \log_{10} M_{\bullet} = +0.23$ ). Greene & Ho (2006) have measured the  $M_{\bullet} - \sigma$  relation in 88 nearby AGN using the photoionization method to determine  $M_{\bullet}$ —the sample is much larger than that of Onken et al. (2004) but the photoionization mass estimates are less direct than those from reverberation mapping. They find  $\Delta \log_{10} M_{\bullet} = -0.21 \pm 0.06$ .

Similarly, Labita et al. (2006) have determined the  $M_{\bullet} - L$  relation from a sample of 29 quasars with  $z < 0.6$ ; they determine black-hole masses using the photoionization method and luminosities using HST photometry. They find  $\Delta \log_{10} M_{\bullet} = -0.36$ , although they interpret their result in terms of recalibrating the photoionization method.

A common feature of the Gebhardt et al. (2000b), Onken et al. (2004), Barth, Greene, & Ho (2005), and Greene & Ho (2006) samples is that their black-hole masses are relatively modest: generally  $M_{\bullet} < 10^8 M_{\odot}$  and often more than an order of magnitude smaller. Selection bias occurs at all  $M_{\bullet}$ , depending on the local slopes of the  $L$  and  $\sigma$  distributions, but these samples are safely removed from the very strong biases seen at large values of  $L$ ,  $\sigma$ , and  $M_{\bullet}$ , where the distribution functions are falling rapidly. Although we have emphasized selection bias in the context of low- and high-redshift samples with similar black-hole masses, one selected by galaxy properties and one by black-hole mass, selection bias can also arise if the two samples are selected in the same way but are centered on different black-hole mass ranges.

We further note that selection effects in these samples are difficult to model—for example, (i) as Gebhardt et al. (2000b) point out, the AGN variability timescale depends on

luminosity, and if the timescale is too long, reverberation mapping is impractical; (ii) to be able to measure the velocity dispersion requires some minimum ratio of the luminosity of the host galaxy to the luminosity of the AGN. If we make the simplest possible assumption, that the samples of nearby galaxies are complete but flux-limited, then equation (32) implies  $\Delta \log_{10} M_{\bullet} = 0.31(\sigma_{\mu}/0.3)^2$ .

Woo et al. (2006), building on the initial work of Treu et al. (2004), examine a sample of 14 Seyfert 1 galaxies at  $z = 0.36 \pm 0.01$ , measuring the velocity dispersions from stellar absorption lines and the black-hole masses by the photoionization method. Compared to the local sample of inactive galaxies with measured black-hole masses, they find  $\Delta \log_{10} M_{\bullet} = 0.62 \pm 0.10 \pm 0.25$ ; note that this result is based on a calibration of the photoionization masses that *assumes* that the Onken et al. (2004) sample should have exactly the same  $M_{\bullet} - \sigma$  relation as inactive galaxies, which need not be the case if selection bias is accounted for. Woo et al. (2006) argue that their offset  $\Delta \log_{10} M_{\bullet}$  is robust because the black-hole masses are measured by the same technique, with the same calibration, in the local and high-redshift samples, but the selection bias in the two samples is likely to be quite different; the Onken et al. (2004) sample is more nearly flux-limited, while the Woo et al. (2006) sample is more nearly luminosity-limited, and the selection bias in these two cases is quite different (eqs. 32 and 25). A useful next step in assessing the bias would be to determine the luminosity function for AGN selected by the criteria used by Woo et al. (2006), for use in equation (25).

It may also be significant that the typical  $M_{\bullet} \approx 4 \times 10^7 M_{\odot}$  in the Onken et al. (2004) sample is roughly an order of magnitude less massive than the typical  $M_{\bullet} \approx 3 \times 10^8 M_{\odot}$  in the Woo et al. (2006) sample. As is evident in Figure 5, the bias is a strong function of  $M_{\bullet}$ , and indeed the bias in the  $M_{\bullet} - \sigma$  relation changes sign at  $M_{\bullet} \sim 10^8 M_{\odot}$ . Thus we would expect that selection bias might affect the results even if the Onken et al. (2004) sample were chosen in precisely the same way as the Woo et al. (2006) sample.

Figure 5 predicts a bias of  $\Delta \log_{10} M_{\bullet} \sim 0.2$  at  $M_{\bullet} \approx 3 \times 10^8 M_{\odot}$  for  $\sigma_{\mu} = 0.30$ . This is only 40% of the offset claimed by Woo et al. (2006). Thus, it appears that selection bias cannot explain all or even most of the Woo et al. (2006)  $\Delta \log_{10} M_{\bullet}$ ; however, given the uncertainties discussed in the previous section, the possibility that the correction may be as large as the claimed offset cannot be ruled out.

Peng et al. (2006) find  $\Delta \log_{10} M_{\bullet} \simeq -0.1$  compared to the local  $M_{\bullet} - L$  relation, using a sample of 11 quasars at  $z \simeq 2$ ; the black-hole masses are determined with the photoionization method. If we assume that the velocity dispersion of the host galaxy does not change between  $z \simeq 2$  and  $z = 0$ , and that the luminosity of the host fades by 1–2 magnitudes as predicted by passive stellar evolution, then this result corresponds to  $\Delta \log_{10} M_{\bullet} \simeq 0.4\text{--}0.8$  as measured by the  $M_{\bullet} - \sigma$  relation. However, the potential selection bias is rather large for this sample,

partly because the cosmic scatter in the  $M_{\bullet} - L$  relation may be larger than in the  $M_{\bullet} - \sigma$  relation. If the sample is luminosity limited, the model shown in the left panel of Figure 5 predicts  $\Delta \log_{10} M_{\bullet} = (0.3-0.7)$  for  $\sigma_{\mu} = 0.5$  for the range of black-hole masses in the sample, and the flux-limited model predicts  $\Delta \log_{10} M_{\bullet} = 0.58$  for  $\sigma_{\mu} = 0.5$  (note that our assumption of a Euclidean metric is not valid at  $z \simeq 2$ , and should be generalized to a realistic cosmological model). A further complication is that their method requires measuring the bulge luminosity in the presence of the bright AGN, so imposes a selection on the ratio of AGN to galaxy luminosity. Without an accurate estimate of the selection bias for the Peng et al. (2006) sample, their measurement of  $\Delta \log_{10} M_{\bullet}$  does not provide clear evidence for rapid evolution in the ratio of black-hole mass to stellar mass in the galaxy.

Salviander et al. (2006) find that galaxies of a given dispersion at  $z \simeq 1$  have black-hole masses that are larger by  $\Delta \log_{10} M_{\bullet} \sim 0.45$  than at  $z \simeq 0$ . In contrast to most other studies, they carefully consider the effects of selection bias using Monte-Carlo models and conclude that for  $\sigma_{\mu} = 0.3$  selection bias increases  $\log_{10} M_{\bullet}$  by  $\sim 0.1$  at low redshift and 0.2 at  $z \simeq 1$ , contributing a net offset of 0.1. They also argue that scatter in the relationship between the width of the [O III] emission line and the true stellar dispersion contributes an additional offset of  $\sim 0.15$ , so after correcting for these biases  $\Delta \log_{10} M_{\bullet} \sim 0.2$ . Their estimates of selection bias are similar to, but somewhat smaller than, the bias that we estimate for their sample from equations (25) and (32), assuming that the low-redshift sample is flux-limited and the high-redshift sample is luminosity-limited; we believe our estimates are more robust because they do not depend on an assumed form for the distribution  $\psi(\lambda - \mu)$  of AGN luminosities at a given black-hole mass.

Finally, we note that theoretical models of the evolution of the  $M_{\bullet} - \sigma$  relation (Robertson et al. 2006) predict  $\Delta \log_{10} M_{\bullet} = -0.18$  at  $z = 2$ . Strong selection bias could reduce or eliminate the difference between this prediction and the positive values of  $\Delta \log_{10} M_{\bullet}$  found at high redshift in most of the above studies.

## 6. Recapitulation

We have described a selection bias that affects investigations into the cosmological evolution of the  $M_{\bullet} - \sigma$  or  $M_{\bullet} - L$  relations. We summarize the main points as follows:

- Cosmic scatter in the  $M_{\bullet} - \sigma$  or  $M_{\bullet} - L$  relations means that a galaxy of given  $L$  or  $\sigma$  will host black holes with a range of  $M_{\bullet}$  values.
- The steep decline in the luminosity function for the most luminous galaxies means that the rare occurrence of high-mass black holes in numerous “modest” galaxies overwhelms

the frequent occurrence of black holes of similar mass in the rare galaxies with very high luminosity. A similar conclusion applies to dispersion instead of luminosity.

- Selection of a sample of black holes hosted by inactive galaxies at low redshift explores the distribution of black-hole masses  $M_{\bullet}$  that a galaxy will host, given its luminosity  $L$  or dispersion  $\sigma$ . Selection of a sample by AGN luminosity at high redshift explores the distribution of  $L$  or  $\sigma$  at a given  $M_{\bullet}$  (if, as is likely, the distribution of AGN luminosity is determined mainly by the black-hole mass rather than the galaxy properties). Confusing the two distributions may create a false signature of evolution.
- The selection bias is substantial for the current estimates of the cosmic scatter in the  $M_{\bullet} - L$  or  $M_{\bullet} - \sigma$  relations, particularly for galaxies containing the most massive black holes. Neither the root-mean-square cosmic scatter nor the shape of the scatter function is known accurately and hence the bias cannot be reliably corrected for, given our present and even foreseeable state of knowledge.
- Our rough estimates of selection bias as applied to a number of evolutionary studies show that the potential bias may be larger than many of the  $\Delta \log_{10} M_{\bullet}$  or  $\Delta s$  values observed. With the notable exceptions of Fine et al. (2006) and Salviander et al. (2006), it appears that most studies of the evolution of the  $M_{\bullet}$  relations have not considered the effects of selection bias. In most cases, accounting properly for selection bias is likely to reduce the the evolution in the  $M_{\bullet}$  relations that has been observed in recent surveys.
- The only way to avoid selection bias is to choose high- and low-redshift galaxy samples using precisely defined, objective criteria that are precisely the same for the two samples. To our knowledge, this has not yet been done.

The work was initiated during a Lorentz Center workshop attended by the authors. We thank the staff of the Lorentz Center and Dr. Tim de Zeeuw for hosting us. We thank Drs. Karl Gebhardt, Richard Green, and Nadia Zakamska for useful conversations.

## REFERENCES

- Barth, A. J., Greene, J. E., & Ho, L. C. 2005, *ApJ*, 619, L151
- Bernardi, M., et al. 2003, *AJ*, 125, 1849
- Bernardi, M., et al. 2006, *AJ*, 131, 2018
- Blanton, M. R., et al. 2003, *ApJ*, 592, 819
- Boyle, B. J., Shanks, T., Croom, S. M., Smith, R. J., Miller, L., Loaring, N., & Heymans, C. 2000, *MNRAS*, 317, 1014
- Dressler, A. 1989, in *IAU Symposium 134, Active Galactic Nuclei*, ed. D. Osterbrock and J. S. Miller (Dordrecht: Kluwer), 217
- Ferrarese, L., & Merritt, D. 2000, *ApJ*, 539, L9
- Fine, S., et al. 2006, *MNRAS*, 373, 613
- Gebhardt, K., et al. 2000a, *ApJ*, 539, L13
- Gebhardt, K., et al. 2000b, *ApJ*, 543, L5
- Gebhardt, K., et al. 2003, *ApJ*, 583, 92
- Greene, J. E., & Ho, L. C. 2006, *ApJ*, 641, L21
- Häring, N. & Rix, H. 2004, *ApJ*, 604, L89
- Hopkins, P. F., Hernquist, L., Cox, T. J., Di Matteo, T., Robertson, B., & Springel, V. 2005, *ApJS*, 163, 1
- Kormendy, J. 1993, in *The nearest active galaxies*, ed. J. Beckman, L. Colina and H. Netzer (Madrid: Consejo Superior de Investigaciones Cientificas), 197
- Kormendy, J., & Richstone, D. 1995, *ARA&A*, 33, 581
- Labita, M., Treves, A., Falomo, R., & Uslenghi, M. 2006, *MNRAS*, 373, 551
- Lauer, T. R., et al. 2007, *ApJ*, 662, 808
- Magorrian, J., et al. 1998, *AJ*, 115, 2285
- Malmquist, K. G. 1924, *Medd. Lund Astron. Obs. Ser. II*, 32, 64

- Novak, G. S., Faber, S. M., & Dekel, A. 2006, *ApJ*, 637, 96
- Onken, C. A., Ferrarese, L., Merritt, D., Peterson, B. M., Pogge, R. W., Vestergaard, M., & Wandel, A. 2004, *ApJ*, 615, 645
- Peng, C. Y., Impey, C. D., Rix, H.-W., Kochanek, C. S., Keeton, C. R., Falco, E. E., Lehár, J., & McLeod, B. A. 2006, *ApJ*, 649, 616
- Postman, M., & Lauer, T. R. 1995, *ApJ*, 440, 28
- Robertson, B., Hernquist, L., Cox, T. J., Di Matteo, T., Hopkins, P. F., Martini, P., & Springel, V. 2006, *ApJ*, 641, 90
- Salviander, S., Shields, G. A., Gebhardt, K., & Bonning, E. W. 2006, *astro-ph/0612568*
- Schechter, P. 1976, *ApJ*, 203, 297
- Sheth, R. K., et al. 2003, *ApJ*, 594, 225
- Shields, G. A., Gebhardt, K., Salviander, S., Wills, B. J., Xie, B., Brotherton, M. S., Yuan, J., & Dietrich, M. 2003, *ApJ*, 583, 124
- Tremaine, S. et al. 2002, *ApJ*, 574, 740
- Treu, T., Malkan, M. A., & Blandford, R. D. 2004, *ApJ*, 615, L97
- Tundo, E., Bernardi, M., Hyde, J. B., Sheth, R. K., & Pizzella, A. 2006, *astro-ph/0609297*
- Yu, Q., & Lu, Y. 2004, *ApJ*, 602, 603
- Yu, Q., & Tremaine, S. 2002, *MNRAS*, 335, 965
- Woo, J.-H., Treu, T., Malkan, M. A., & Blandford, R. D. 2006, *ApJ*, 645, 900

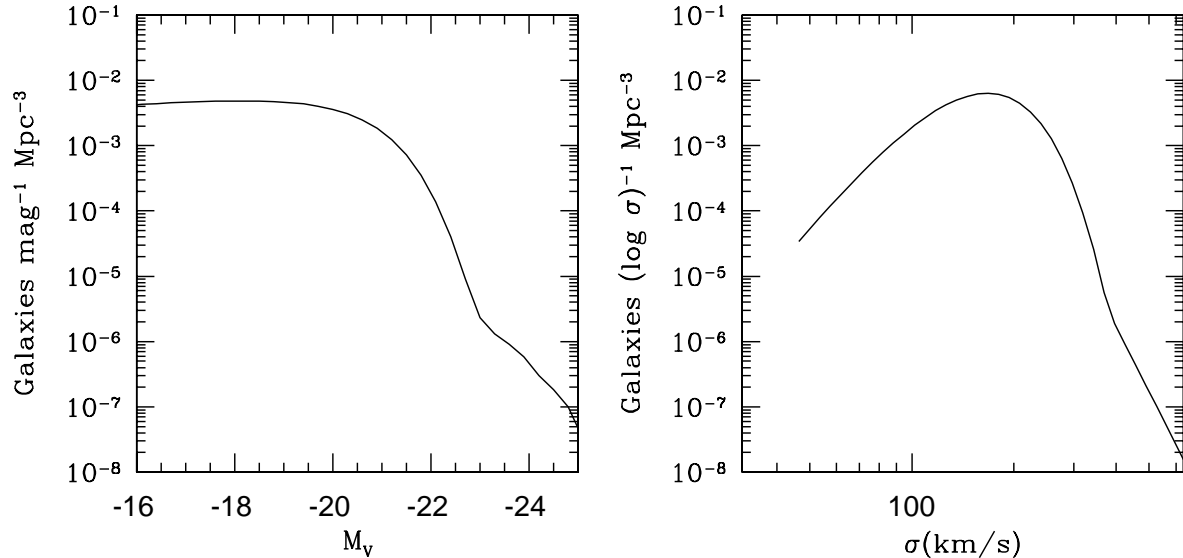


Fig. 1.— The number density of galaxies as a function of luminosity (left) and velocity dispersion (right), assuming  $H_0 = 70 \text{ km s}^{-1} \text{ Mpc}^{-1}$ . The luminosity function is based on data from the Sloan Digital Sky Survey (Blanton et al. 2003), augmented at large luminosities by the Postman & Lauer (1995) sample of brightest cluster galaxies. The velocity-dispersion function is based on SDSS data (Sheth et al. 2003), augmented at large dispersions by the sample identified by Bernardi et al. (2006). See Lauer et al. (2007) for details.

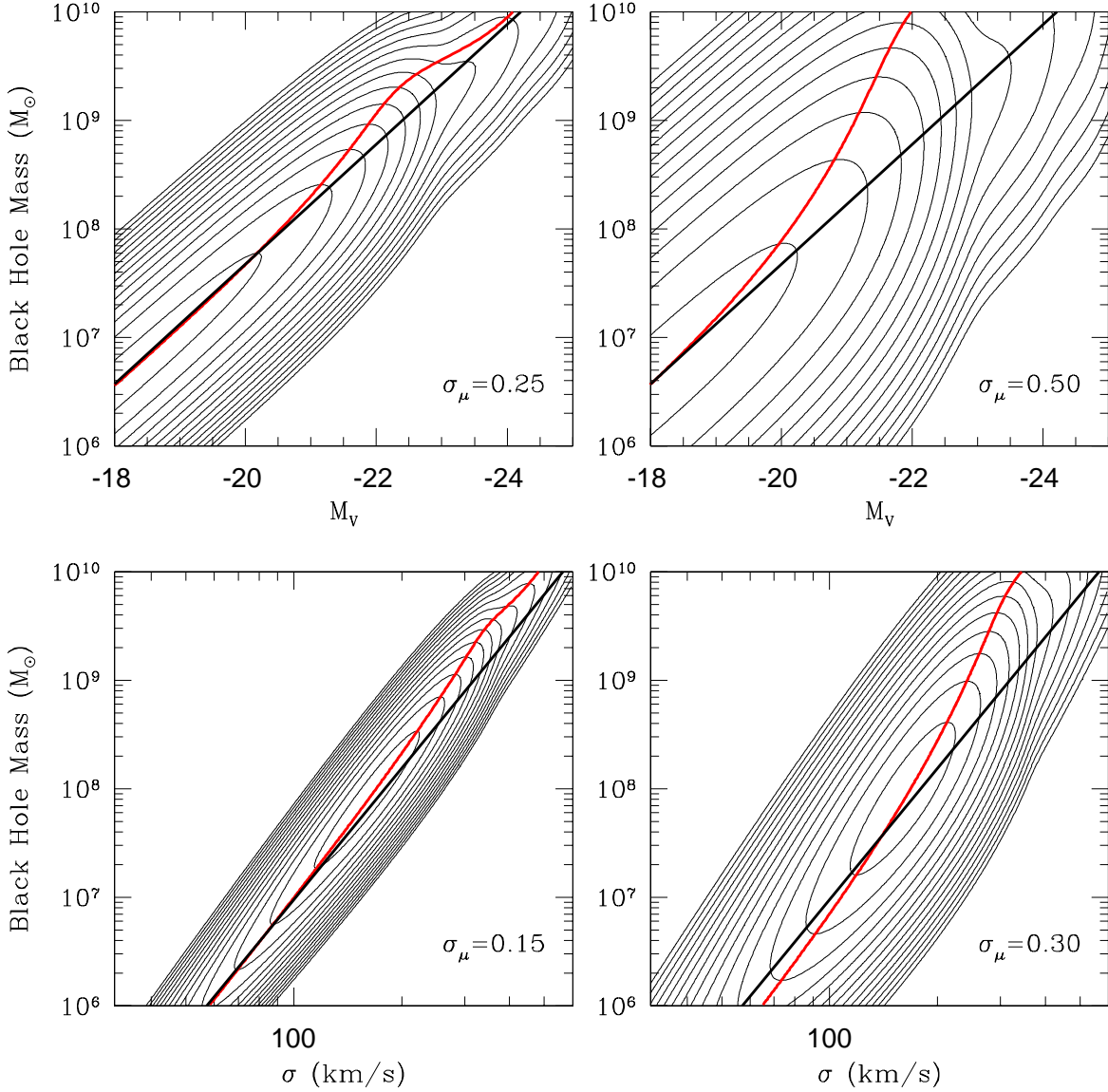


Fig. 2.— The joint probability distribution of galaxy luminosity  $L$  (top panels) or stellar velocity dispersion  $\sigma$  (bottom panels) and black-hole mass,  $M_{\bullet}$ . The solid, straight, black line gives the mean  $M_{\bullet} - L$  or  $M_{\bullet} - \sigma$  relation (eqs. 4 and 5). The joint distribution is calculated by assuming that the black-hole mass has a log-normal distribution about the  $M_{\bullet} - L$  or  $M_{\bullet} - \sigma$  relation, with the normalization provided by the galaxy luminosity or velocity-dispersion functions shown in Figure 1. The adopted dispersions in  $\log_{10} M_{\bullet}$  are  $\sigma_{\mu} = 0.25, 0.50$  for the  $M_{\bullet} - L$  relation or  $\sigma_{\mu} = 0.15, 0.30$  for the  $M_{\bullet} - \sigma$  relation. The contours are arbitrary, but are spaced in increments of 0.5 dex in density. The curved red lines give the mean  $M_V$  or  $\log_{10}(\sigma)$  as a function of  $M_{\bullet}$ . The displacement of this line from the mean relations gives the bias at a given  $M_{\bullet}$ .

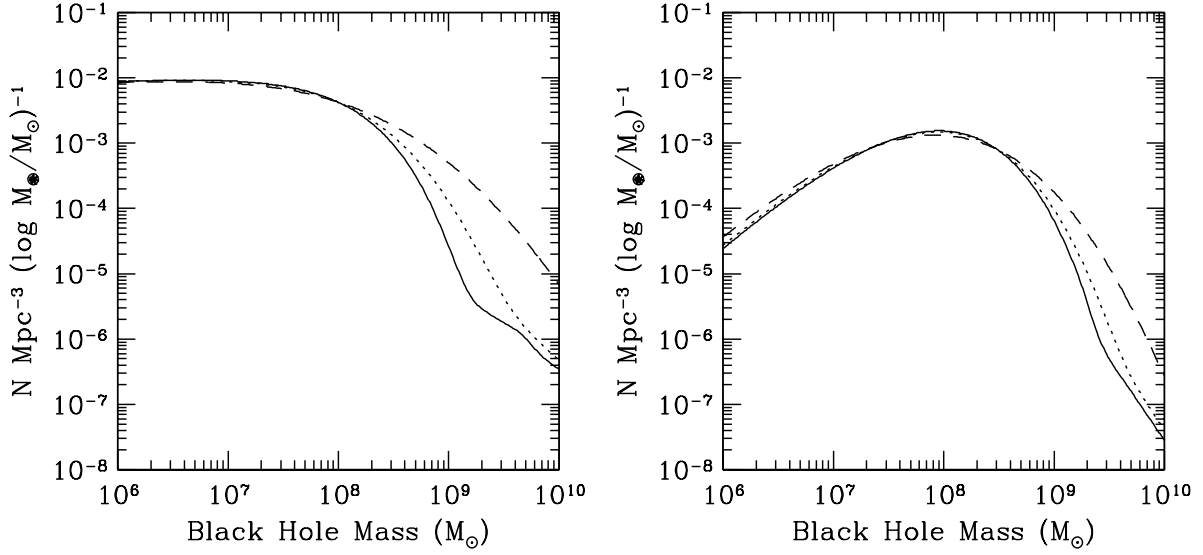


Fig. 3.— The effects of cosmic scatter in the  $M_{\bullet} - \sigma$  or  $M_{\bullet} - L$  relations on the number density of black holes as a function of  $M_{\bullet}$ . The left panel is based on the  $M_{\bullet} - L$  relation of equation (5) combined with the luminosity function of Figure 1. The right panel is based on the  $M_{\bullet} - \sigma$  relation of equation (4) combined with the velocity-dispersion function of Figure 1. Solid lines show the results assuming no scatter in the  $M_{\bullet}$  relations, while the dashed lines show the effects of increasing amounts of cosmic scatter  $\sigma_{\mu}$ . The dotted and dashed lines show the effects of  $\sigma_{\mu} = 0.25, 0.50$  for the  $M_{\bullet} - L$  relationship and  $\sigma_{\mu} = 0.15, 0.30$  for the  $M_{\bullet} - \sigma$  relationship. Cosmic scatter greatly enhances the volume density of black holes at the high-mass end.

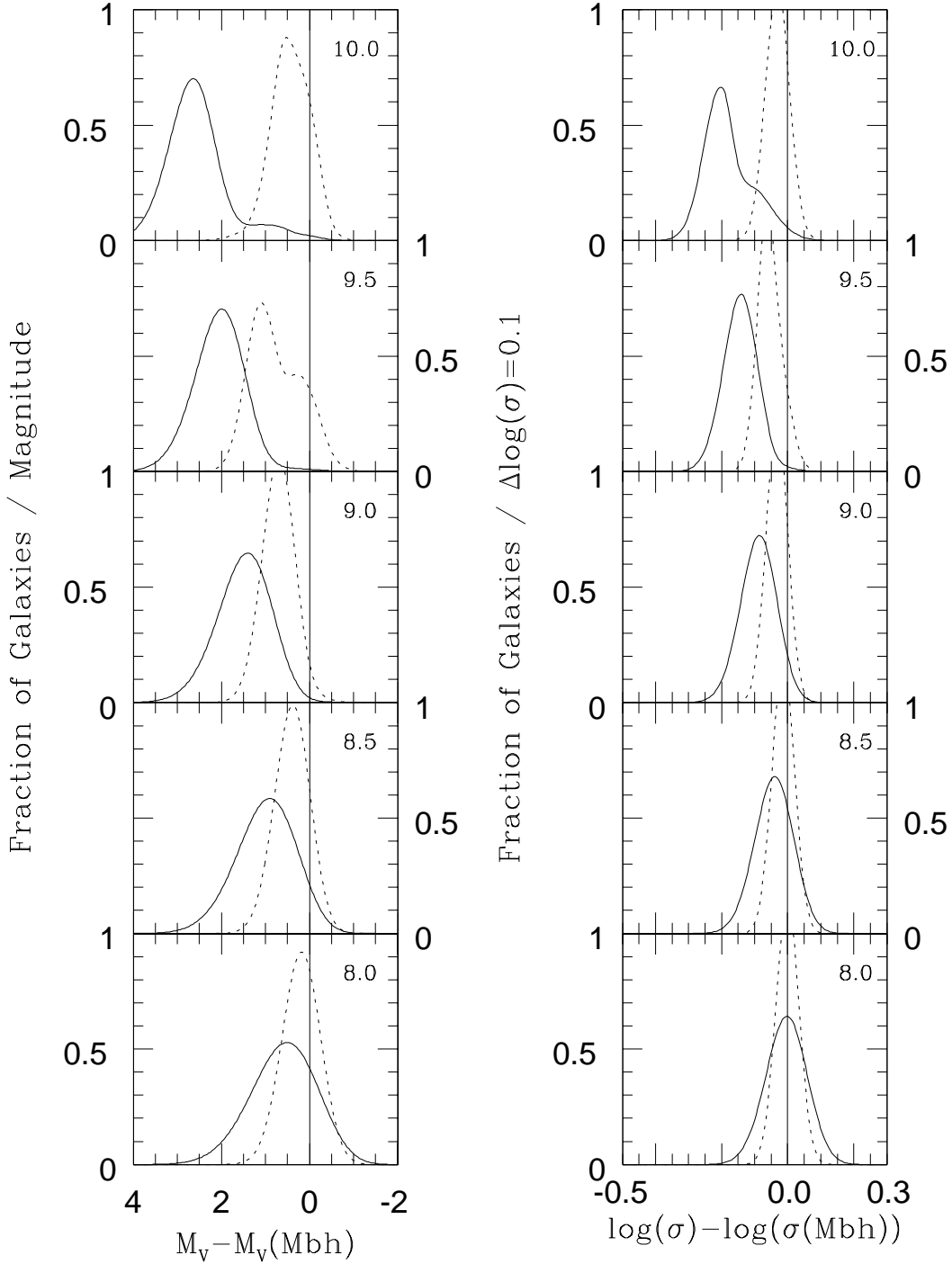


Fig. 4.— The distribution of absolute magnitude  $M_V = -2.5 \log_{10} L + \text{const}$  or velocity dispersion  $\log_{10} \sigma$  at selected values of  $M_\bullet$  ( $\log_{10} M_\bullet / M_\odot$  is given in the upper right of each panel). These probability distributions are obtained by taking horizontal cuts through the joint distributions shown in Figure 2, and are appropriate when the sample selection is on black-hole mass. Two distributions are shown with dashed and solid lines, corresponding respectively to  $\sigma_\mu = 0.25, 0.50$  for  $M_V$  on the left or  $\sigma_\mu = 0.15, 0.30$  for  $\log_{10} \sigma$  on the right. The horizontal coordinate is the difference between either  $M_V$  or  $\log_{10} \sigma$  and the nominal values  $f^{-1}(s)$  determined from the  $M_\bullet - L$  or  $M_\bullet - \sigma$  relations (4) and (5).

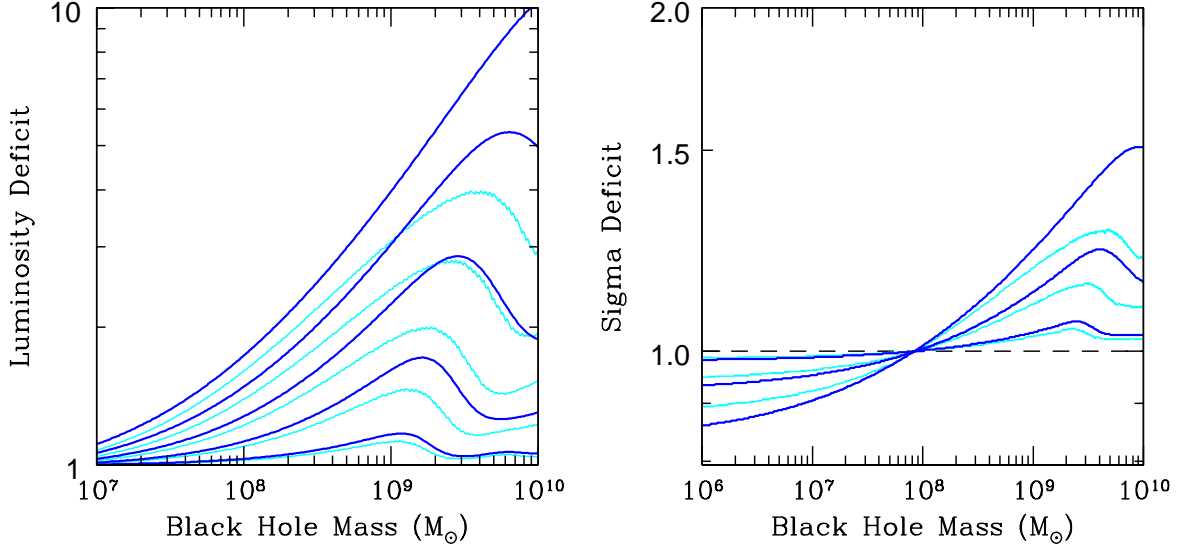


Fig. 5.— The ratio of the nominal values  $f^{-1}(s)$  determined from the  $M_{\bullet} - L$  or  $M_{\bullet} - \sigma$  relations to  $\langle s \rangle_{\mu}$ , the mean of  $\log_{10} L$  or  $\log_{10} \sigma$  at a given black-hole mass. This Figure quantifies the bias in a sample selected by  $M_{\bullet}$  as opposed to  $s$ . The blue curves are drawn for  $\sigma_{\mu} = 0.1, 0.2, \dots, 0.5$  for  $\log_{10} L$  (left panel), and  $\sigma_{\mu} = 0.1, 0.2, 0.3$  for  $\log_{10} \sigma$  (right panel). The cyan curves show the biases that result if the assumed normal distributions in  $\log_{10} M_{\bullet}$  (eq. 7) are truncated at  $\pm 2\sigma_{\mu}$ . At high  $M_{\bullet}$  the bias depends not only on the amplitude of the cosmic scatter, but also on the form of the wings of the scatter function.

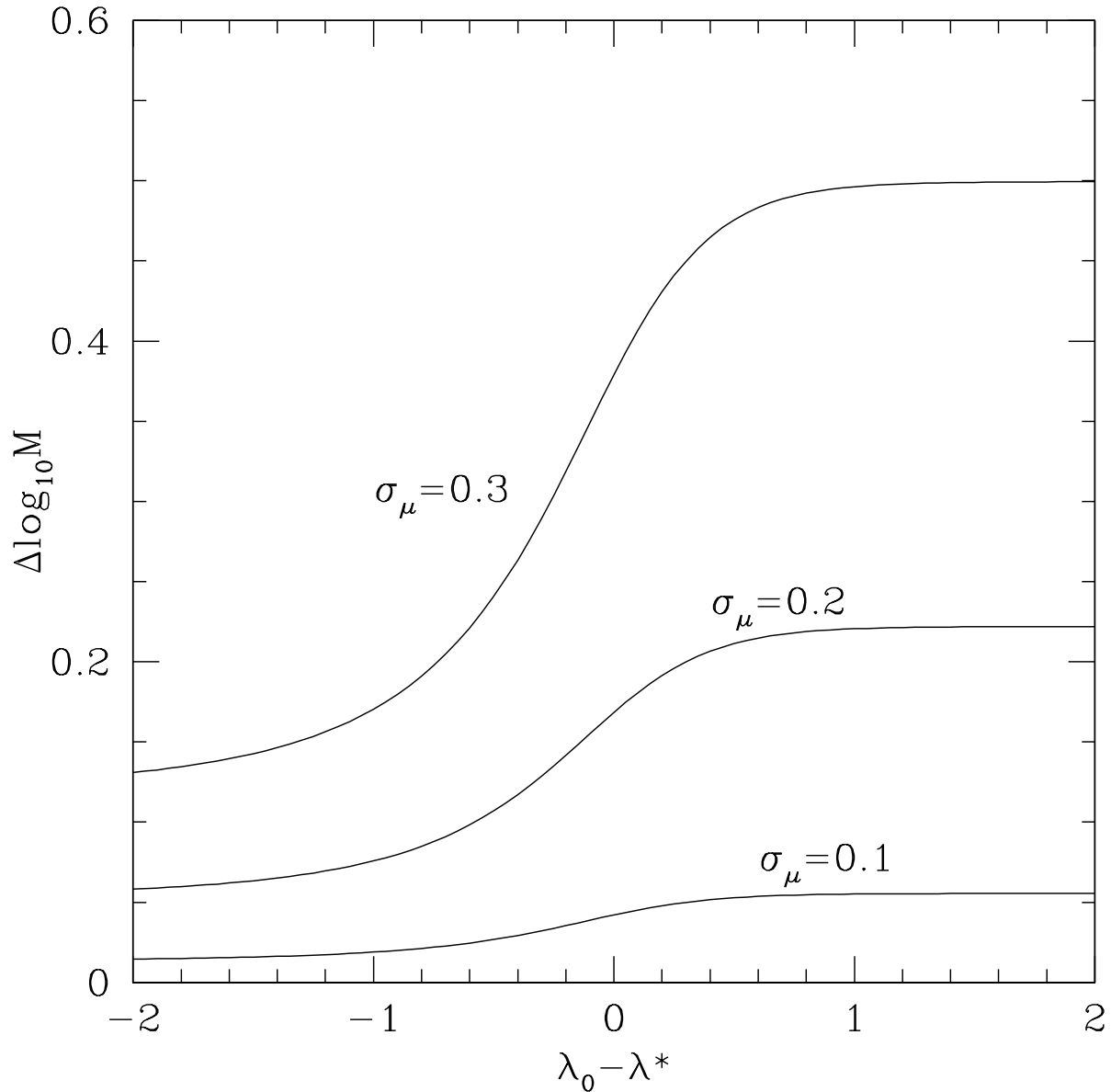


Fig. 6.— The bias in  $\log_{10} M_\bullet$  from the  $M_\bullet - \sigma$  relation for inactive galaxies in a luminosity-limited survey of AGN. The horizontal axis is  $\lambda_0 - \lambda^* = \log_{10}(L_0/L^*)$  where  $L_0$  is the limiting luminosity at the survey redshift and  $L^*$  is the break luminosity of the AGN luminosity function (26).